High Mobility, Air-Stable Organic Transistors from Hexabenzocoronene/Carbon Nanotube Bilayers†

Kenneth D. Harris,‡,§ Shengxiong Xiao,§ Chang Young Lee,|| Michael S. Strano,|| Colin Nuckolls,§ and Graciela B. Blanchet*,‡

DuPont Central Research and Development, Wilmington, Delaware 19880, Department of Chemistry, Columbia University, New York, New York 10027, Department of Chemical and Biomolecular Engineering, University of Illinois at Urbana−Champaign, Urbana, Illinois 61801

Received: March 8, 2007; In Final Form: August 28, 2007

The pick-up-stick transistor concept is demonstrated using materials that are both air-stable and fully solution processable. In this paper, the thin film transistor (TFT) semiconductor is a bilayer structure with an array of carbon nanotubes (CNTs) as an underlayer and an alkyl-substituted hexabenzocoronene (HBC) overcoat. Electrical current flowing through the structure favors the low resistance CNTs, and therefore, the effective channel length, transconductance, and charge carrier mobility are modulated by the CNT density. With this structure, we measure a field effect mobility of 0.1 cm^2/Vs which represents a factor of 6 improvement over that of HBC without a CNT underlayer. All fabrication is carried out in a bright, air-filled environment.

Introduction

Research in organic electronics is primarily guided by the desire to inexpensively manufacture a variety of electronic devices such as RFID labels, displays, and memory storage devices.[1−3] Although the operational figures of merit for organic devices are not expected to match those of contemporary inorganic materials,[4−6] organic semiconductors offer significant processing and manufacturing advantages. Organic electronics research has, therefore, primarily been an effort to achieve adequate electrical properties, while processing in an ambient environment using high throughput techniques such as inkjet, thermal transfer, or reel-to-reel printing.[7−11]

In a soluble semiconductor, the parameter most commonly used to evaluate device performance is the charge carrier mobility (μ), and considerable research has focused on developing semiconductor molecules with increasingly large intrinsic mobilities. Greater values lead to a wider range of available switching frequencies, yet from a device standpoint, it is not fully accurate to attribute this effect solely to the intrinsic charge carrier mobility. Geometric factors including the channel length (L), channel width (W), and gate capacitance (C_i) as well as the driving voltage (V_{sd}) play equally critical roles, and a parameter incorporating many of these quantities is the transconductance, g_m.[6] The transconductance is related to the charge carrier mobility by the following formula:

$$g_m = \frac{\partial I_d}{\partial V_g} \cong \mu C_i \left(\frac{W}{L}\right) V_{sd} \quad (1)$$

Although charge carrier mobility is indeed important, increasing the channel width/length ratio also linearly increases the transconductance, and therefore, channel length reduction, as in high-resolution photolithographic approaches, is also a viable path to improved performance. Unfortunately, the cost of photolithography is prohibitive in high volume production, and therefore, the poor resolution of commercial printing techniques (currently in the range 20−50 μm) becomes the primary factor preventing the production of inexpensive organic electronic devices. The situation can be improved, however, by printing composite materials entirely within the equipment resolution limits, which operate as if they had reduced effective channel lengths. This is the essence of the "pick-up-stick transistor" concept.[12]

In a pick-up-stick transistor, a pure organic semiconductor with a known charge carrier mobility is combined with a high conductivity, large aspect ratio material, such as carbon nanotubes (CNTs). This two-component semiconductor is applied to a substrate and provided with source, drain, and gate electrodes in a typical thin film transistor (TFT) geometry (Figure 1a). Electrical interfaces between CNTs and a number of organic semiconductors have previously been shown to create exceptionally low resistance contacts,[13,14] and therefore, composite devices are expected to benefit from low contact resistance. In our case, the CNTs and semiconductor are applied in a bilayer configuration, and three situations of interest occur as the density of nanotubes in the underlayer is increased.[15] At low densities (Figure 1c), the effective channel length is somewhat reduced by short-circuiting through the CNTs, but the charge carrier mobility remains largely determined by that of the semiconducting component. In this regime, a gradual increase in performance is expected with increasing CNT density. For large CNT densities (Figure 1e), interconnected nanotubes provide numerous low-resistance routes between source and drain electrodes. Under these circumstances, the organic semiconductor has little influence over the electrical properties of the composite, and the measured parameters are essentially equivalent to random CNT networks.[16−18] The target of the pick-up-stick transistor concept lies between the two extremes (Figure 1d). In this situation, a large fraction of the channel is electrically short-circuited by nanotubes, yet finite gaps remain which are filled with semiconductor. Any gaps near

† Part of the special issue "Richard E. Smalley Memorial Issue".
* To whom correspondence should be addressed.
‡ DuPont Central Research and Development.
§ Columbia University.
|| University of Illinois at Urbana−Champaign.

10.1021/jp071898i CCC: $37.00
Published on Web 10/11/2007

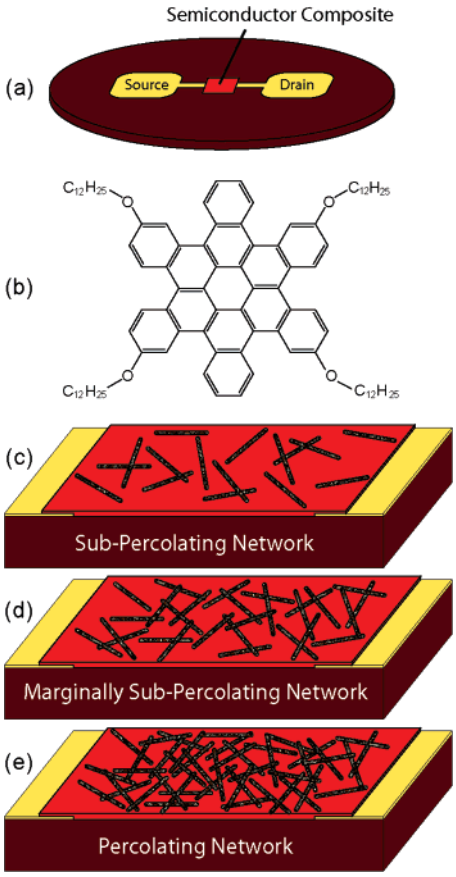

Figure 1. In the "pick-up-stick" transistor concept, the semiconductor of a conventional organic transistor is replaced by a two-component composite (a). In our case, the materials are tetraoxydodecyl-substituted hexabenzocoronene (b), and carbon nanotubes. Three situations of interest occur as the concentration of nanotubes is increased: sub-percolating networks (c), marginally sub-percolating networks (d), and fully percolating networks (e).

the dielectric interface may be switched by gate voltage modulation and become the active component of the transistor. Under these circumstances, we expect a transconductance significantly greater than that of the pure organic semiconductor, together with an on/off current ratio that remains large.

The pick-up-stick concept was first demonstrated with homogeneous CNT/polythiophene (P3HT) composites and with a CNT/pentacene system in a bilayer configuration.[19,20] In each case, large improvements in transconductance and carrier mobility were measured; however, these particular semiconductors do have certain disadvantages when considering a scale-up to high throughput printed electronics. Pentacene, for example, was deposited under vacuum, whereas P3HT was handled under dark, low-oxygen conditions. In this paper, we investigate the pick-up-stick concept using tetraoxydodecyl-substituted hexabenzocoronene (HBC, Figure 1b) as the organic semiconductor.[21−26] This compound is highly advantageous due to its air-stability and processability from organic solutions, both of which are properties critical to applications in low cost printed electronics.

Results and Discussion

Hexabenzocoronene. The HBC semiconductor was synthesized and purified using a previously reported technique.[21] At room temperature and in the pure state, the raw semiconductor is a yellow/orange compound that is readily soluble in chloroform and shows little propensity toward photooxidation in air. Crystallographic studies have predicted a monoclinic structure with unit cell parameters $a = 24.414(4)$ Å, $b = 19.764(3)$ Å, $c = 8.7374(16)$ Å, and $\beta = 96.984(5)°$. X-ray diffraction (XRD) spectra of thin films spun from chloroform solution (see Figure 2a) are dominated by the group of peaks at $2\theta \approx 3.7°$, 7.3°, 11.2°, 14.9°, and 18.6°, corresponding to multiple reflections at a d spacing of 24 Å. This value agrees closely with the measured periodicity along the a-axis, and we can assign the set of peaks to the (h00) crystal planes. Few additional features are present in the XRD spectra. The broad peaks centered at roughly $2\theta \approx 27°$ and 42° do not markedly vary with processing conditions and can be assigned to scattering in the amorphous glass substrate. The absence of any additional (hkl) reflections from the HBC semiconductor allows us to partially determine the crystal orientation and place the a axis roughly normal to the substrate surface. Periodicity in this direction is 24 Å, while charge transfer is more likely to occur by transverse core-to-core hopping along an axis lying in the plane on the film.

The intensity of the XRD peaks varies strongly with processing conditions, with the most intense spectrum collected for a sample prepared on a pretreated glass substrate (i.e., the substrate was immersed in a 0.1 M solution of octadecyltrichlorosilane (OTS) in toluene for 30 min prior to the application of the HBC semiconductor) and annealed (for 1 h at 250 °C before cooling at 1 °C/min to room temperature) following spin-coating. This spectrum is shown in Figure 2a. (OTS pretreatment is thought to provide a low surface energy substrate which limits molecule/surface interactions, encourages crystallinity, and provides a degree of orientation control.) The evolution of crystallinity in the HBC semiconductor, as inferred from intensity variation in the (200) ($2\theta = 7.3°$) peak, is tracked in the inset of Figure 2a. Substrate surface treatments and postdeposition anneals clearly improve crystallinity, and higher performance TFTs are expected from these samples. Although temperatures as high as 250 °C are not strictly compatible with printed electronics in many applications, significant improvements in crystallinity are also observed using more modest anneal temperatures. The (200) intensity, for instance, increased from 35 to 640 counts when an OTS treatment and anneal at 140 °C were used (Figure 2a, inset), and both treatments are compatible with fabrication on flexible PET substrates.

The ability of the HBC compound to self-organize is also reflected in its UV−vis absorption spectra (shown in Figure 2b), as strong bathochromic shifts are readily observed between solution and thin film forms. The primary peaks in the range 2.9−3.5 eV are assigned to various vibronic ($\pi \rightarrow \pi^*$) excitations within the HBC core,[27] and each is red-shifted more than 0.1 eV when the system is transferred to the solid state. Surface treatments and anneal steps, which enable increased crystallinity as measured by XRD, also drive small additional bathochromic shifts (e.g., a ~0.02 eV shift is observed between the curves in the inset of Figure 2b), and therefore, we can correlate an increased crystallinity with a concomitant reduction in the $\pi \rightarrow \pi^*$ band gap.

Carbon Nanotubes. Critical to this study is the ability to achieve well dispersed carbon nanotube suspensions without degrading the electrical properties. Although many surfactants effectively disperse CNTs, most are also insulating materials with energy barriers prohibitive to electrical conduction. In our case, HiPco single-walled CNT precursors[28] were individually suspended in a 1 wt % sodium dodecyl sulfate (SDS) aqueous solution via sonication followed by ultra-centrifugation.[29,30] The CNT solution, flocculated by acetone, was then filtered while rinsing with methanol to remove SDS. The solid material was

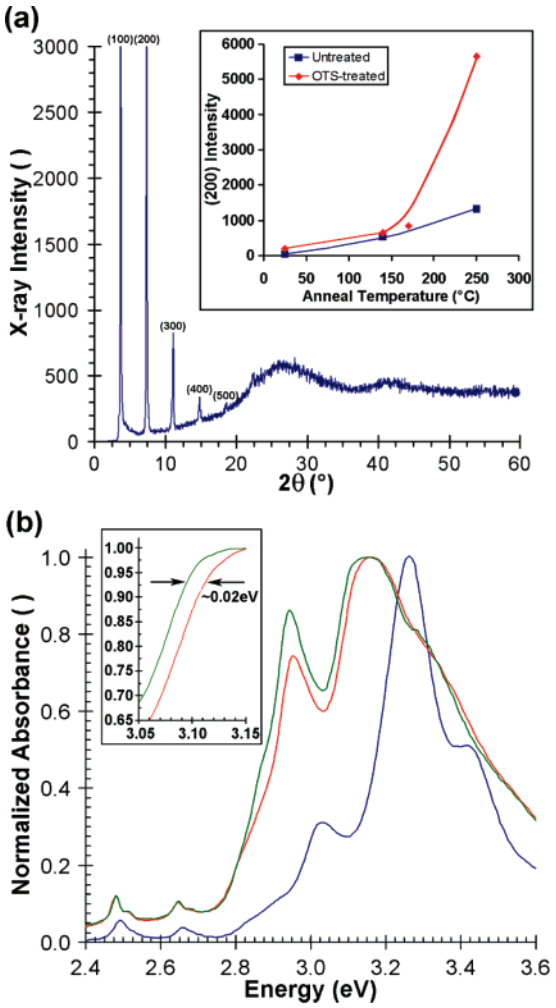

Figure 2. Analysis of the HBC material. (a) XRD spectrum for HBC spin-cast onto an OTS-treated substrate and annealed at 250 °C. The intensity variation for the (200) $2\theta = 7.3°$ peak under various processing conditions is shown in the inset. (b) UV−vis absorption spectra for HBC in (1 wt %) chloroform solution (blue), as a thin film without surface treatment or annealing (red), and as a thin film with both surface treatment and anneal cycle (green). A limited region is magnified in the inset.

then dried and re-dispersed in an aromatic organic solvent (ortho-dichlorobenzene, oDCB). At this stage, the mixture consists of 200 mg/L individual single-wall carbon nanotubes in suspension with oDCB. Before application to a substrate, the stock mixture was generally diluted with varying quantities of oDCB to adjust the CNT density in the final film. An atomic force microscope (AFM) image of a CNT film spin-cast at 1000 rpm from a 20 mg/L CNT dispersion in oDCB is shown in Figure 3a.

TFT Fabrication. TFTs were fabricated on heavily doped silicon wafers with a 3000 Å thermal oxide. Gold source and drain electrodes were lithographically patterned on one wafer face, and a gate electrode was applied on the other. In all cases, we employ large channel dimensions ($W = 200$ μm, $L = 20$ μm) which are appropriate considering the end application as inexpensive printed electronics. The wafer surface was OTS-treated for 30 min prior to application of the semiconductor components. The CNT/HBC semiconductor composite was applied in a bilayer configuration, and all processing was performed under ambient environmental conditions. The CNTs (dispersed with varying concentrations in oDCB) were spin-cast at 1000 rpm and dried at 65 °C. HBC was applied directly onto CNT-coated substrates by spin-coating (from 1 wt %

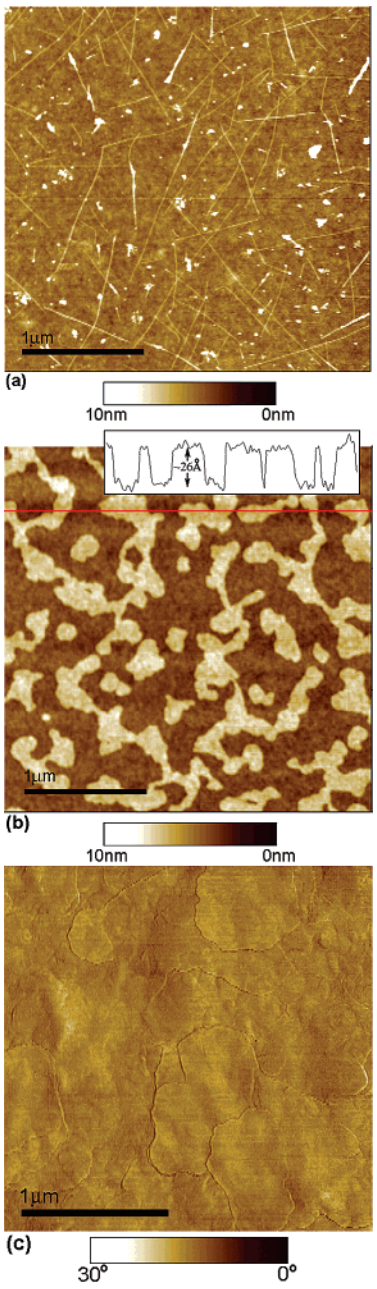

Figure 3. AFM images of CNT and CNT/HBC bilayers. Carbon nanotubes spun from a 20 mg/L dispersion are shown in panel a, and a thin HBC film spin-cast over a similar CNT-coated substrate is shown in panel b. A height profile for the points along the red line is provided in the inset of panel b, and the 26 Å steps are in good agreement with the *d*-spacings observed by XRD. In panel c, an AFM phase image in shown in a 150 nm thick region.

chloroform solution) at 1000 rpm. The samples were dried at 65 °C, annealed in air at 250 °C for 1 h, and cooled at 1 °C/min to room temperature. AFM images of HBC/CNT bilayers are included as Figure 3, panels b and c, and in the images, HBC is continuous over the entire frame, with no CNTs or areas of the Si substrate visible. Figure 3b shows a region of thin HBC where an incomplete monolayer has formed above several complete layers. A surface profile (along the red line) is shown in the inset, and sharp boundaries can be observed between layers. The measured height differences across a number of these boundaries were tabulated and generally found to occur in discrete multiples of ~26 Å, a value which corresponds with that of the 24 Å *d* spacing observed by XRD. This suggests that the disordered CNT underlayer does not disrupt the

crystallinity of the HBC and that its semiconducting properties may be preserved in the bilayer structure. In Figure 3c, the surface of a ~150 nm sample is shown in a phase image, and large crystal platelets remain visible in this thickness range.

Electrical Measurements. Electrical properties of the HBC semiconductor, CNT arrays and CNT/HBC bilayers were measured using a three terminal TFT characterization technique. A gate capacitance of 11.5 nF/cm^2 was used in all calculations (i.e., a value equivalent to 300 nm of thermal silicon oxide). Source and drain electrodes were energized with $V_{ds} = -80$ V, and the gate voltage was swept from +20 V to −80 V, while measuring the drain current (I_d). Without CNTs, field effect mobilities measured for the pure HBC compound were on the order of 0.01 cm^2/Vs. (Rather than reporting transconductance values, most authors report field effect mobilities inferred from plots of I_d vs V_g, and therefore, we also report field effect mobilities calculated using the procedure outlined previously.)[21] The maximum value achieved without CNTs was 0.016 cm^2/Vs, and this value will be used as the baseline for all comparisons with HBC/CNT bilayers. For CNT layers measured before application of an HBC overcoat, no appreciable drain current or gating effect was observed in samples prepared from low concentration CNT dispersions (below ~20 mg/L). Above percolation, the electrical properties of a CNT network become strongly concentration dependent. With a CNT concentration of 50 mg/L (i.e., well above the percolation threshold), an average effective mobility of 0.5 cm^2/Vs was measured over eight 200 μm x 20 μm devices, and the accompanying average on/off current ratio was 50. In the past, some TFTs based on percolated CNT networks have shown significantly greater field effect mobilities; in a number of cases, values as large as 40 cm^2/Vs have been reported.[31,32] In these devices, CNTs were generally grown by chemical vapor deposition (CVD) and patterned by transfer-printing, and their improved field effect mobility suggest that the performance of hybrid devices may potentially be improved using similar materials and methods.

Using the pick-up-stick concept, it was found that the semiconducting properties of the HBC system were considerably improved with the addition of a CNT underlayer in the near-percolation regime. In Figure 4a, a plot of the effective mobility and on/off ratio measured for numerous CNT/HBC bilayer devices is shown. In the figure, the concentration noted is that of dispersed carbon nanotubes spin-cast to form the underlayer. Due to the semirandom nature of the CNT spin, the semiconductor parameters for the CNT/HBC system cannot be fully predicted from the initial concentration of nanotubes, but strong statistical trends are apparent in the data. With nanotube concentrations greater than approximately 30 mg/L in oDCB, the devices have measured effective mobilities greater than 0.1 cm^2/Vs and on/off ratios below 10. In the lowest concentration regime, below approximately 20 mg/L, little change is observed from the behavior of the pure HBC. No obvious variation in the on/off ratio, and only a gradual increase in effective mobility with increasing CNT content are recorded. In the intermediate concentration range (20−30 mg/L), rapid variation is measured. This concentration regime is associated with CNT densities near the onset of percolation and represents the target of the pick-up-stick transistor concept. The majority of our best performing samples were fabricated from CNT concentrations in this range.

In order to map the field effect mobilities for individual devices to their associated on/off ratios, the parameters for each CNT/HBC device are directly plotted against one another in Figure 4b. With 10^4 taken as a minimum acceptable on/off ratio limit, mobility values on the order of 0.1 cm^2/Vs are represented

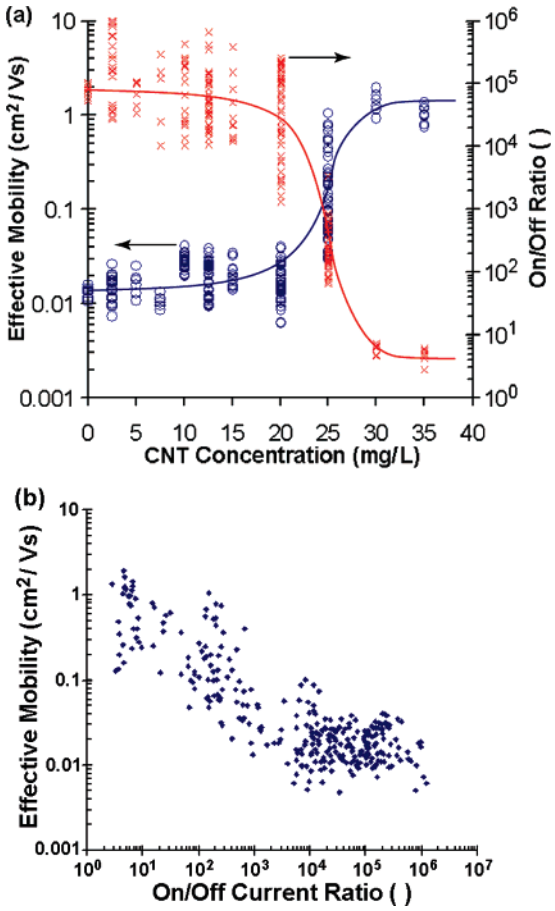

Figure 4. (a) Effective mobility (blue circle) and on/off ratio (red X) of CNT/HBC bilayer TFTs as a function of CNT concentration during spin coating. A sharp transition in the range 20-25 mg/L reflects the onset of percolation. (b) The range of effective mobility and on/off ratio values measured for individual CNT/HBC bilayer devices.

in Figure 4b. Compared to the 0.016 cm^2/Vs established for the best pure HBC devices, this represents a factor of 6 improvement over bulk HBC devices and pushes the HBC/CNT system into the range of values achieved for P3HT.[4] The P3HT compound, which is generally considered among the best-performing semiconductors processable from solution, must be handled under low-oxygen conditions to preserve acceptable mobilities, and therefore HBC/CNT systems carry a significant advantage in that processing and device fabrication is possible in an ambient environment.

Conclusions

By embedding high conductivity carbon nanotubes beneath an organic semiconductor (HBC), the transconductance and charge carrier mobility of the semiconductor have been significantly improved. For the CNT/HBC system, the effective mobility was increased by a factor of 6 while preserving on/off ratios above 10^4. In addition, the semiconductor/conductor combination of HBC/CNT has the particularly advantageous feature that all processing was completed in an air environment, and no special precautions regarding the ambient lighting were required. This renders the composite attractive in low-cost electronics applications.

Acknowledgment. The authors thank Dennis Redmond and Will Marshall for X-ray measurements and Nancy Tassi for processing and AFM support. We also acknowledge the Columbia Nanocenter for financial support. M.S.S. acknowl-

edges a CAREER Award from the National Science Foundation (Grant No. CTS-0449147) and funding from Intel (Class A). M.S.S is also grateful for a 2004 DuPont Young Investigator Award.

References and Notes

(1) Rogers, J. A.; Bao, Z.; Baldwin, K.; Dodabalapur, A.; Crone, B.; Raju, V. R.; Kuck, V.; Katz, H.; Amundson, K.; Ewing, J.; Drzaic, P. *Proc. Natl. Acad. Sci. U.S.A.* **2001**, *98*, 4835.

(2) Sirringhaus, H.; Tessler, N.; Friend, R. H. *Science* **1998**, *280*, 1741.

(3) Dimitrakopoulos, C. D.; Malenfant, P. R. L. *Adv. Mater.* **2002**, *14*, 99.

(4) Shaw, J. M.; Seidler, P. F. *IBM J. Res. Dev.* **2001**, *45*, 3.

(5) Leong, M.; Doris, B.; Kedzierski, J.; Rim, K.; Yang, M. *Science* **2004**, *306*, 2057.

(6) Muller, D. A. *Nat. Mater.* **2005**, *4*, 645.

(7) *Organic Electronics, Materials, Manufacturing and Applications*; Klauk, H., Ed.; Wiley-VCH: Weinheim, 2006.

(8) Bao, Z. N.; Rogers, J. A.; Katz, H. E. *J. Mater. Chem.* **1999**, *9*, 1895.

(9) Dimitrakopoulos, C. D.; Mascaro, D. J. *IBM J. Res. Dev.* **2001**, *45*, 11.

(10) Forrest, S. R. *Nature* **2004**, *428*, 911.

(11) Blanchet, G. B.; Loo, Y. L.; Rogers, J. A.; Gao, F.; Fincher, C. R. *Appl. Phys. Lett.* **2003**, *82*, 463.

(12) Blanchet, G. B.; Bo, X. Z.; Lee, C. Y.; Strano, M. S.; Nuckolls, C. *Solid State Comm.* **2005**, *135*, 638.

(13) Cao, Q.; Zhu, Z. T.; Lemaitre, M. G.; Xia, M. G.; Shim, M.; Rogers, J. A. *Appl. Phys. Lett.* **2006**, *88*.

(14) Lefenfeld, M.; Blanchet, G.; Rogers, J. A. *Adv. Mater.* **2003**, *15*, 1188.

(15) Kumar, S.; Blanchet, G. B.; Hybertsen, M. S.; Murthy, J. Y.; Alam, M. A. *Appl. Phys. Lett.* **2006**, *89*, 143501.

(16) Snow, E. S.; Novak, J. P.; Campbell, P. M.; Park, D. *Appl. Phys. Lett.* **2003**, *82*, 2145.

(17) Xiao, K.; Liu, Y. Q.; Hu, P. A.; Yu, G.; Wang, X. B.; Zhu, D. B. *Appl. Phys. Lett.* **2003**, *83*, 150.

(18) Ko, H.; Tsukruk, V. V. *Nano Lett.* **2006**, *6*, 1443.

(19) Bo, X. Z.; Tassi, N. G.; Lee, C. Y.; Strano, M. S.; Nuckolls, C.; Blanchet, G. B. *Appl. Phys. Lett.* **2005**, *87*, 203510.

(20) Bo, X. Z.; Lee, C. Y.; Strano, M. S.; Goldfinger, M.; Nuckolls, C.; Blanchet, G. B. *Appl. Phys. Lett.* **2005**, *86*, 182102.

(21) Xiao, S. X.; Myers, M.; Miao, Q.; Sanaur, S.; Pang, K. L.; Steigerwald, M. L.; Nuckolls, C. *Angew. Chem., Int. Ed.* **2005**, *44*, 7390.

(22) Xiao, S. X.; Tang, J. Y.; Beetz, T.; Guo, X. F.; Tremblay, N.; Siegrist, T.; Zhu, Y. M.; Steigerwald, M.; Nuckolls, C. *J. Am. Chem. Soc.* **2006**, *128*, 10700.

(23) Guo, X. F.; Myers, M.; Xiao, S. X.; Lefenfeld, M.; Steiner, R.; Tulevski, G. S.; Tang, J. Y.; Baumert, J.; Leibfarth, F.; Yardley, J. T.; Steigerwald, M. L.; Kim, P.; Nuckolls, C. *Proc. Natl. Acad. Sci. U.S.A.* **2006**, *103*, 11452.

(24) Iyer, V. S.; Wehmeier, M.; Brand, J. D.; Keegstra, M. A.; Mullen, K. *Angew. Chem., Int. Ed.* **1997**, *36*, 1604.

(25) Pisula, W.; Menon, A.; Stepputat, M.; Lieberwirth, I.; Kolb, U.; Tracz, A.; Sirringhaus, H.; Pakula, T.; Mullen, K. *Adv. Mater.* **2005**, *17*, 684.

(26) Schmidt-Mende, L.; Fechtenkotter, A.; Mullen, K.; Moons, E.; Friend, R. H.; MacKenzie, J. D. *Science* **2001**, *293*, 1119.

(27) Cohen, Y. S.; Xiao, S. X.; Steigerwald, M. L.; Nuckolls, C.; Kagan, C. R. *Nano Lett.* **2006**, *6*, 2838.

(28) Carbon Nanotechnologies Inc., Houston, TX.

(29) Strano, M. S.; Moore, V. C.; Miller, M. K.; Allen, M. J.; Haroz, E. H.; Kittrell, C.; Hauge, R. H.; Smalley, R. E. *J. Nanosci. Nanotechnol.* **2003**, *3*, 81.

(30) O'Connell, M. J.; Bachilo, S. M.; Huffman, C. B.; Moore, V. C.; Strano, M. S.; Haroz, E. H.; Rialon, K. L.; Boul, P. J.; Noon, W. H.; Kittrell, C.; Ma, J. P.; Hauge, R. H.; Weisman, R. B.; Smalley, R. E. *Science* **2002**, *297*, 593.

(31) Cao, Q.; Xia, M. G.; Shim, M.; Rogers, J. A. *Adv. Funct. Mater.* **2006**, *16*, 2355.

(32) Zhou, Y. X.; Gaur, A.; Hur, S. H.; Kocabas, C.; Meitl, M. A.; Shim, M.; Rogers, J. A. *Nano Lett.* **2004**, *4*, 2031.